IN VITRO HEPATIC OXIDATIVE BIOTRANSFORMATION OF TRIMETHOPRIM

BY

JENNIFER LYNN GOLDMAN

Submitted to the graduate degree program in Clinical Research and the Graduate Faculty of the University of Kansas in partial fulfillment of the requirements for the degree of Master of Science.

Chairperson Theresa I. Shireman, PhD, RPh

J. Steven Leeder PharmD, PhD

Gregory L. Kearns PharmD, PhD

Date Defended: March 23, 2015

The Thesis Committee for Jennifer Lynn Goldman
certifies that this is the approved version of the following thesis:

IN VITRO HEPATIC OXIDATIVE BIOTRANSFORMATION OF TRIMETHOPRIM

Chairperson Theresa Shireman, PhD, RPh

Date approved: March 23, 2015

ABSTRACT

Introduction: Trimethoprim-sulfamethoxazole (TMP-SMX) is a commonly used antibiotic often associated with idiosyncratic adverse drug reactions (IADRs). Historically, bioactivation of SMX to a reactive intermediate has been implicated in IADRs. Recently, the bioactivation of TMP has been described as TMP *N*-acetyl cysteine (NAC) adducts were identified following human liver microsome (HLM) incubations and in the urine of children taking TMP, suggesting cytochrome P450 enzymes (P450s) catalyze TMP bioactivation. In this study, we identified the P450s involved in the formation of six TMP primary metabolites.

Methods: A panel of characterized HLMs (n=16), c-DNA expressed P450s, and pooled HLMs in the presence and absence of selective P450 inhibitors were incubated with therapeutic concentrations of TMP. Reactive metabolites were trapped with NAC, and metabolite formation was quantified by UPLC/MS/MS. Correlation coefficients between the rates of metabolite formation and P450 marker reaction rates were determined using least-squares regression analysis and evaluated at α=0.05.

Results: 1-NO-TMP, Cα-NAC-TMP and Cα-OH-TMP were formed by CYP3A4 and inhibited by ketoconazole (CYP3A inhibitor). 4'-demethylation was catalyzed by several P450s including CYP3A4, correlated with multiple CYPs, and inhibited primarily with ketoconazole suggesting CYP3A4 contributed to 4'-demethylation. 3-NO-TMP was formed by CYP1A and inhibited by α-naphthoflavone (CYP1A inhibitor). 3'-demethylation was catalyzed by multiple P450s including CYP2C9, correlated with CYP2C9 activity and inhibited by sulphafenazole (CYP2C9 inhibitor).

Conclusion: These findings suggest that P450s were responsible for the primary metabolism of TMP with CYPs 2C9 and 3A4 being the most significant contributors to TMP primary metabolism. Factors modulating activity of these enzymes may affect the risk of IADRs.

ACKNOWLEDGEMENTS

I would like to acknowledge my committee members Drs. Theresa Shireman, J. Steven Leeder and Gregory L. Kearns for their guidance during conduct of this work and my thesis development. I would also like to acknowledge the work of my colleagues and collaborators Drs. Leon Van Haandel and Robin Pearce for their support in completion of this work. Financial support was provided by a Children's Mercy Hospital Marion Merrell Dow Internal Grant and the National Center for Advancing Translational Sciences KL2TR000110.

TABLE OF CONTENTS

INTRODUCTION

Trimethoprim-sulfamethoxazole (TMP-SMX) is a frequently prescribed antimicrobial for the treatment of urinary tract, skin and soft tissue infections, and the prevention opportunistic infections in the immune-compromised host (Copp et al., 2011; Hersh et al., 2008; Mofenson et al., 2009). This drug combination is also one of the most common causes of unpredictable, undesired and potentially severe idiosyncratic adverse drug reactions (IADRs) that include rash, fever, lymphadenopathy, cytopenias, liver injury or severe skin detachment (Stevens Johnson Syndrome or toxic epidermal necrolysis) (Roujeau et al., 1995; Clarkson and Choonara, 2002). Historically, SMX has been suspected as the inciting agent in these IADRs, largely based on its ability to form a nitroso intermediate capable of modifying proteins resulting in subsequent immunogenicity and antigenicity (Manchanda et al., 2002; Naisbitt et al., 2002). However, administration of TMP alone has also been associated with severe and even fatal IADRs (Hawkins et al., 1993; Mortimer et al., 2005; Nwokolo et al., 1988). We recently identified *N*-acetyl cysteine (NAC) adducts of TMP metabolites in the urine of children taking TMP-SMX, confirming bioactivation *in* vivo, and raising the possibility that TMP may contribute to IADRs (van Haandel et al., 2014). Incubations containing human liver microsomes (HLMs), NAC and an NADPH-generating system formed all of the TMP-NAC adducts observed in urine, suggesting the possibility that cytochrome P450 enzymes (P450s) may catalyze TMP bioactivation.

TMP is largely excreted unchanged in the urine. Several stable human urinary metabolites have previously been identified: the *N*-oxides, 1-NO-TMP and 3-NO-TMP, which are generated by oxidation of nitrogen atoms in the pyrimidine ring; the benzylic alcohol, Cα-OH-TMP, formed via oxidation of the methylene bridge; and 3' and 4'-desmethyl-TMP resulting

from oxidative *O*-demethylation (Figure 1) (Brooks et al., 1973; Sigel et al., 1973). *In vitro* data generated by Damsten et al, suggest that multiple *O*-demethylation reactions may occur, resulting in up to three free hydroxyl groups on the benzylic ring (Damsten et al., 2008).

In addition to the formation of these stable metabolites, evidence of TMP bioactivation has been demonstrated *in vitro* through the trapping of bioactivated TMP metabolites with small molecular weight thiols, such as NAC. TMP reactive metabolites are believed to form through both direct oxidation to an imino-quinone methide and via sequential secondary oxidation of primary, demethylated TMP metabolites to form a quinone methide (Damsten et al., 2008; Lai et al., 1999). Consistent with this *in vitro* evidence for TMP bioactivation, we detected six NAC-TMP conjugates in the urine of children taking TMP-SMX (van Haandel et al., 2014).

In vitro results have demonstrated that TMP bioactivation is catalyzed by P450s, although the specific enzymes involved in generating both the stable and reactive metabolites have not been well defined. Damsten et al described the formation of several NAC adducts and stable metabolites from TMP utilizing HLMs, rat liver microsomes, heterologously expressed P450 enzymes and P450 BM3 mutants. Based only on data from incubations containing heterologously expressed human P450s 1A2, 2C8, 2C9, 2C19, 2D6, 2E1 and 3A4, Damsten et al suggested that CYP1A2 and CYP3A4 were capable of forming the imino-quinone, while CYP2D6 was primarily responsible for catalyzing both the demethylation and subsequent secondary oxidation step to the quinone-methide species, and CYP3A4 catalyzed multiple TMP demethylation reactions leading to quinone methide intermediates (Damsten et al., 2008). Unfortunately, additional studies, such as correlation analyses with marker P450 activities in a panel of HLMs and inhibition of metabolite formation with P450 selective inhibitors, were not

performed to more fully characterize the quantitative importance of individual P450s. Formation of reactive intermediates, such as the imino-quinone and quinone methide species, are believed to be the initiating step in IADRs; thus, the aim of this study was to characterize the role of the P450s involved in the formation of TMP primary stable and reactive metabolites at therapeutically relevant concentrations of TMP to identify the enzymes most likely to contribute to TMP bioactivation at pharmacologically relevant exposures. Defining the metabolic pathways leading to the bioactivation of TMP is a critical first step to better understand factors that may contribute to variability in reactive metabolite formation, and potentially, the risk of developing IADRs.

MATERIALS AND METHODS

Chemicals

LC-MS Optima® grade water, methanol, and acetonitrile were purchased from Fisher Scientific (FairLawn, NJ, USA). EDTA, formic acid (LC-MS grade), glucose-6-phosphate dehydrogenase, magnesium chloride, N-acetyl-L-cysteine, NADP, potassium phosphate dibasic, potassium phosphate monobasic, TMP, α-Naphthoflavone, tranylcypromine, montelukast, sulfaphenazole, quinidine, 4-methylpyrazole, and danazol were obtained from Sigma Aldrich Chemical Co. (St. Louis, MO). Benzylnirvanol, and thiotepa were purchased from Toronto Research Chemicals (Toronto, Ontario, Canada). Ketoconazole was obtained from Research Biochemicals International (Natick, MA). All reagents were reagent grade quality or higher. 1-NO-TMP, 3-NO-TMP, 4'-desmethyl-TMP, Cα-OH-TMP, and Cα-NAC-TMP were custom synthesized by Artis-Chem Co. Ltd (Shanghai, China). Purity of the standards was determined to be ≥98% by H-NMR, LCMS and LCUV at 214nm.

Human Liver Microsomes and cDNA-Expressed Enzymes

A reaction phenotyping kit (Version 8; containing HLMs prepared from16 individuals; 4 females, 12 males), pooled HLMs, and EasyCYP Bactosomes (manufactured by Cypex Ltd, Scotland, UK) were purchased from XenoTech, LLC (Lenexa, KS). The EasyCYP bactosomes included the following cDNA-expressed human P450 enzymes: P450s 1A1, 1A2, 1B1, 2A6, 2A13, 2B6, 2C8, 2C9, 2C18, 2C19, 2D6, 2E1, 2J2, 3A4, 3A5, 3A7 and 4A11. Microsomes were stored at -80°C and placed on ice prior to use.

***In vitro* incubation conditions**

Standard *in vitro* enzyme incubations (200-µl) contained HLMs (20 µg of microsomal protein) or bacculovirus cDNA-expressed P450 enzymes (4 pmol), potassium phosphate buffer (50mM, pH 7.4), $MgCl_2$ (3mM), EDTA (1mM), NAC (5mM) and TMP (0-500 µM) dissolved in water. Reactions were initiated by the addition of a NADPH-generating system consisting of NADP (1 mM), glucose 6-phosphate (1 U/ml), and glucose-6-phosphate dehydrogenase (5mM). Following the addition of NADPH, reactions were incubated in a shaking water bath at 37 ± 1°C for 0-30 minutes, and were terminated by the addition of 200 µL of ice-cold methanol. Protein was precipitated by centrifugation at 10,000 g for 10 minutes and an aliquot of supernatant was analyzed by HPLC/MS via direct injection.

Preliminary experiments with TMP (0.5, 0.75, 1, 2.5, 5, 7.5, 10, 25, 50, 75, 100, 250, 300, 400, 500 µM) and pooled HLMs (0.1, 0.5, 1.0 mg protein/ml) suggested that the rates of TMP metabolite formation were proportional to protein concentration (1.0 mg/ml) and time (60 min). Under these conditions, TMP biotransformation was less than 15%. Correlation experiments with HLMs were performed in triplicate with two replicate samples per condition.

Kinetic experiments and experiments performed with cDNA-expressed P450s were conducted in duplicate.

Chemical-Inhibition Experiments

Conversion of TMP (50 μM) to the primary metabolites of interest (1-NO-TMP, 3-NO-TMP, 3'-desmethyl-TMP, 4'-desmethyl-TMP, Cα-OH-TMP, and Cα-NAC-TMP) by pooled HLMs was determined in the presence or absence of selective, competitive P450 inhibitors at four concentrations encompassing the denoted ranges including: α-Naphthoflavone (CYP1A2, 0.15-5 μM), tranylcypromine (CYP2A6, 0.2-6 μM), thiotepa (CYP2B6, 5-150 μM), montelukast (CYP2C8, 0.15-5 μM), sulfaphenazole (CYP2C9, 0.3-10 μM), benzylnirvanol (CYP2C19, 0.3-10 μM), quinidine (CYP2D6, 0.15-5 μM), 4-methylpyrazole (CYP2E1, 2-60 μM), danazol (CYP2J2, 0.02-0.6 μM), and ketoconazole (CYP3A4, 0.03-1 μM). These ranges of inhibitor concentrations were based on reported Ki values with the highest concentration of inhibitor approximately ~30 times Ki (range: Ki, 3 Ki, 10 Ki and 30 Ki). Inhibition experiments were conducted in triplicate with replicates.

UPLC MS/MS Analysis

Sample analysis was performed by UPLC MS/MS, as described by (van Haandel et al., 2014). Optimization of the analysis protocol included the injection of 3μL of sample to minimize band broadening, and the custom synthesis of reference compounds. The availability of reference standards allowed us to construct calibration curves for 1-NO-TMP, 3-NO-TMP, 4'-desmethyl-TMP, Cα-OH-TMP, and Cα-NAC-TMP. 3'-desmethyl-TMP was quantitated from the 4'-desmethyl-TMP standard because of its structural similarity and due to the absence of available reference material. Calibration curves were constructed in MeOH quenched

incubations containing HLMs and 1, 3, 10, 30, 100, 300 or 400 μM concentrations of standard reference compounds.

Data Analysis

Correlation coefficients (r) between the rates of 1-NO-TMP, 3-NO-TMP, 3'-desmethyl-TMP, 4'-desmethyl-TMP, Cα-OH-TMP, and Cα-NAC-TMP formation with the known expressed activities of P450 enzymes in the HLM reaction phenotype kit were determined using least-squares regression analysis to evaluate the relationship between enzymatic activity and metabolite formation. Significance was determined by Pearson's regression analysis using a two-tailed t-test with $\alpha = 0.05$ (JMP® 10). Effects of the selective P450 inhibitors were determined by comparing the rate of individual metabolite formation as per cent of control by inhibitor concentration (Microsoft Excel 2007®). Rate calculations with the heterologously expressed enzymes were corrected for metabolite formation by microsomes containing vector only. Data derived from kinetic incubation studies using HLMs and selected c-DNA expressed enzymes (CYP2C9 and 3A4) were analyzed by nonlinear regression to estimate K_m and V_{max} values. These data were visually inspected via Eadie–Hofstee and Lineweaver-Burk plots and subsequently fit to a one-enzyme Michaelis-Menten model (GraphFit 5; Erithacus Software Ltd., Surrey, UK).

RESULTS

Biotransformation of TMP by HLMs

Incubations containing HLMs (pooled and from individual donors), TMP (5 and 50 μM) and NAC catalyzed the formation of six primary metabolites from TMP, namely, 1-NO-TMP, 3-NO-TMP, 3'-desmethyl-TMP, 4'-desmethyl-TMP, Cα-OH-TMP, and Cα-NAC-TMP (Figure 1).

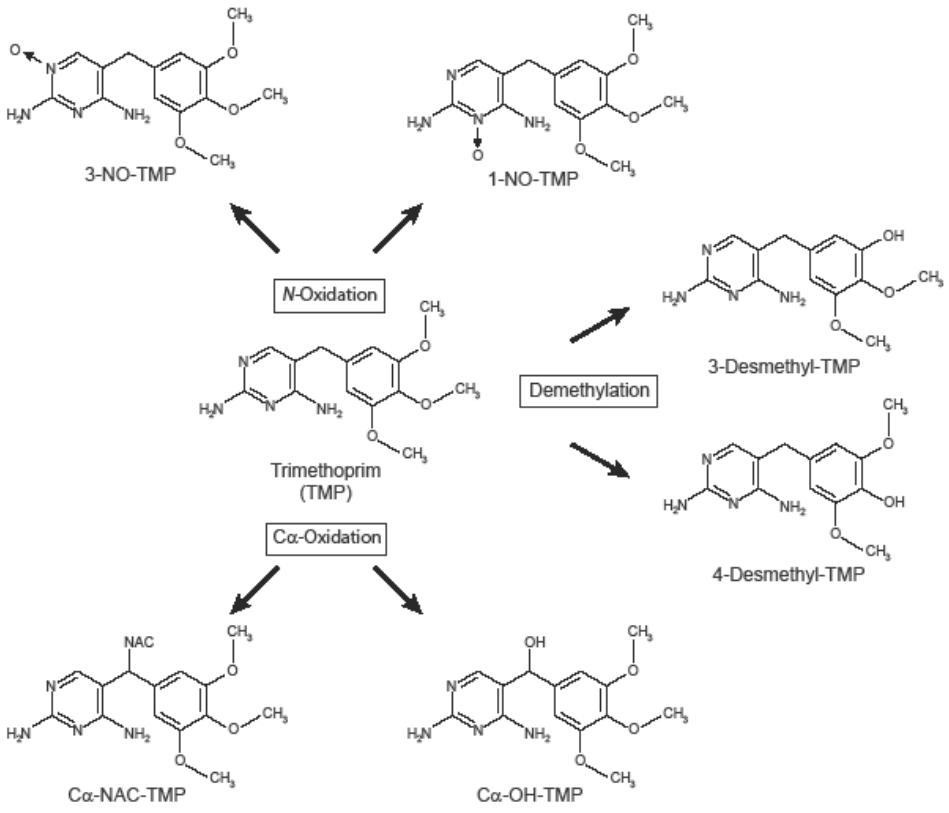

Figure 1. Metabolic scheme for the conversion of TMP to its primary oxidative metabolites.

Formation of these metabolites was consistent with our previous *in vitro* and in *vivo* observations (van Haandel et al., 2014). The 3'- and 4'-desmethyl-TMP were the most abundant metabolites present and accounted for approximately 65 and 25 percent of the total metabolite formation, respectively, regardless of substrate concentration. Of the remaining metabolites, only 1-NO-TMP had an abundance approaching 5 per cent; each of the other minor metabolites constituted less than 2 per cent of the total metabolite formation (Figure 2).

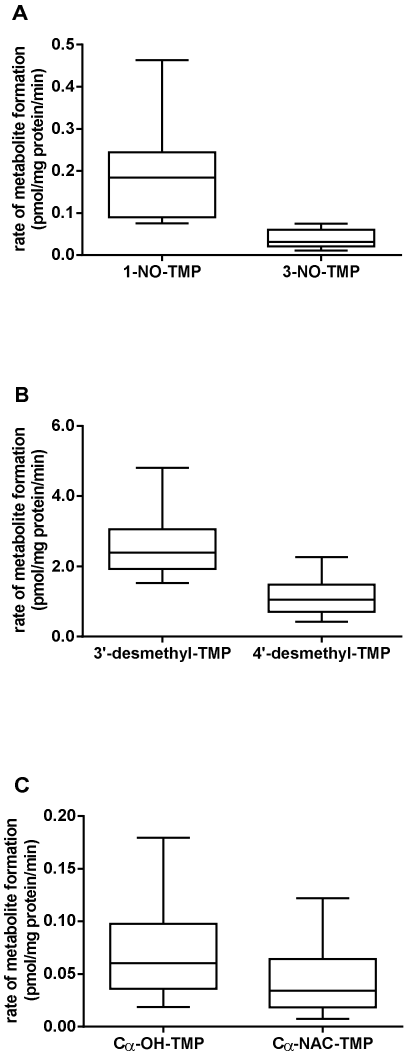

Figure 2. Variability in the rate of formation of primary trimethoprim formation.

Metabolism by flavin-containing monooxygenases (FMOs) was evaluated with heat inactivation of FMOs by heating pooled HLMs at 45°C for 5 minutes prior to incubations. There was no evidence of FMO contributing to primary TMP metabolism.

The kinetics of formation for the six primary TMP metabolites were estimated in pooled adult HLMs and in microsomes containing cDNA-expressed CYP2C9 and CYP3A4 enzymes (Table 1).

Table 1. Estimated kinetic parameters for the formation of TMP primary metabolites in human liver microsomes and cDNA-expressed human P450 enzymes

	Km [a]	**Vmax** [b,c]	Cl_{int} [d,e]
Pooled HLMs			
1-NO-TMP	1050 ± 120	69 ± 6	0.07
3-NO-TMP	690 ± 76	5 ± 0.3	0.007
3'-desmethyl-TMP	647 ± 55	453 ± 25	0.70
4'-desmethyl-TMP	482 ± 42	146 ± 7	0.30
Cα-OH-TMP	2180 ± 400	108 ± 17	0.05
Cα-NAC-TMP	1310 ± 160	18 ± 2	0.01
CYP 2C9			
1-NO-TMP	531 ± 264	23.3 ± 6.87	0.044
3-NO-TMP	428 ± 253	5.97 ± 1.95	0.014
3'-desmethyl-TMP	1330 ± 400	2030 ± 470	1.53
4'-desmethyl-TMP	I.D.	I.D.	I.D.
Cα-OH-TMP	I.D.	I.D.	I.D.
Cα-NAC-TMP	I.D.	I.D.	I.D.
CYP 3A4			
1-NO-TMP	971 ± 188	1320 ± 190	1.36
3-NO-TMP	N.D.	N.D.	N.D.
3'-desmethyl-TMP	1470 ± 510	2060 ± 571	1.40
4'-desmethyl-TMP	1040 ± 231	1430 ± 240	1.38
Cα-OH-TMP	754 ± 122	1020 ± 110	1.35
Cα-NAC-TMP	784 ± 143	137 ± 18	0.17

N.D. metabolite not detected

I.D. insufficient data to determine kinetic parameters

Value ± S.E. [a]micromolar, [b]pmol/mg protein per minute for pooled HLMs, [c]pmol/nmol P450/min for heterologously expressed enzymes, [d] µl/mg protein per minute for pooled HLMs, [e]µl /nmolP450 per minute for heterologously expressed

CYP2C9 and CYP3A4 were selected as it is thought that both significantly contribute to either direct bioactivation of TMP (Cα-NAC-TMP) or result in the abundant formation of primary metabolites (3' and 4'-desmethyl-TMP) that could potentially undergo further bioactivation to potential reactive species. The aqueous solubility of TMP limited final incubation concentrations to 500 μM or less. Direct plots of substrate concentration versus rate of TMP metabolite formation indicated that substrate saturation did not occur for the formation of any of the TMP primary metabolites (i.e., the plateau phase was not achieved). Although this precluded an accurate estimation of K_m and V_{max} parameters, Eadie-Hofstee plots were constructed for the available data. While there was a slight indication of substrate activation in the formation of Cα-OH-TMP, visual inspection of the Eadie-Hofstee plots for each of the six primary metabolites suggested that they could be fit to a single-enzyme Michaelis-Menten equation. Data were then fit to a single enzyme model using the software, Grafit 5, to estimate the kinetic parameters K_m and V_{max}, which are shown in Table 1. Of note, all of the determined K_m values for the six primary metabolites were above 450 μM, and as high as 2 mM, markedly higher than therapeutic concentrations of TMP observed *in vivo*. These conditions are such that the enzyme is not the rate-limiting factor for TMP biotransformation and ensures conditions for first-order kinetics.

TMP N-oxidation (1 and 3-NO-TMP)

Incubations with microsomes containing one of seventeen cDNA-expressed human P450 enzymes were conducted at two TMP concentrations (5μM and 50 μM) to evaluate the ability of these enzymes to catalyze formation of the TMP N-oxides. The selected TMP concentrations were based on observed *in vivo* TMP $C_{max.}$(Hoppu and Arjomaa, 1984; Rylance et al., 1985)

Several heterologously expressed P450 enzymes, including CYP1A1, CYP1B1, CYP2C19, CYP3A4, CYP3A5 and CYP3A7, were capable of catalyzing 1-NO-TMP formation (Figure 3, panel A, 5μM data shown) while CYP1A1 and CYP1B1 were the heterologously expressed enzymes that catalyzed the highest rates of 3-NO-TMP formation.

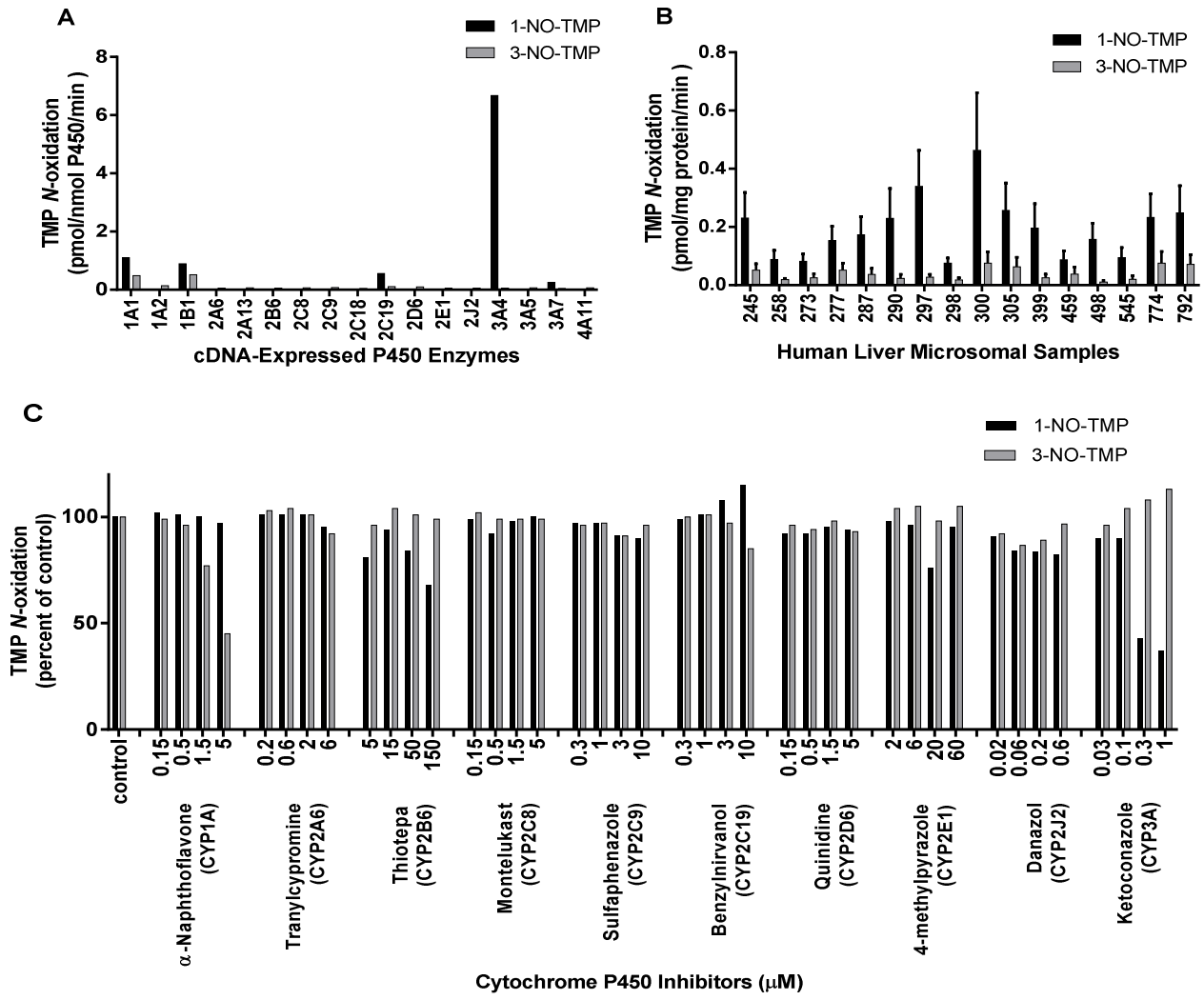

Figure 3. *N*-oxidation of TMP to primary metabolites.

A panel of HLMs prepared from 16 individual donors and characterized for P450 and FMO activities using marker substrate reactions was examined for the ability to catalyze formation of TMP 1- and 3-*N*-oxides from TMP. Each of the microsomal preparations catalyzed the formation of both *N*-oxides to various degrees. At a substrate concentration of 5 μM, the rate of TMP *N*-oxide formation varied >6-fold;1-*N*-oxide formation (rates ± S.D.) ranged from 0.08 ± 0.02 to 0.46 ± 0.20 pmol/mg protein/min whereas 3-*N*-oxide formation ranged from 0.01 ± 0.005 to 0.08 ± 0.04 pmol/mg protein/min (Fig 2, panel A; Figure 3, panel B). Rates of TMP 1- and 3-*N*-oxide formation for each of the microsomal samples increased proportionally (approximately) with a 10-fold increase in substrate concentration (50 μM; results not shown). The sample-to-sample variation in the rates of 1-NO-TMP formation, correlated significantly ($P< 0.01$) with CYP2A6, CYP2C8, CYP2C9, and CYP3A4 activities whereas 3-NO-TMP formation correlated significantly with CYP1A2, CYP2C8 and CYP2C9 activities, but not with any other P450 or FMO activities (Table 2).

Table 2. Correlation analysis (r) of the relationship between the rates of TMP primary metabolite formation with the sample-to-sample variation in cytochrome P450 activities in human liver microsomes

Cytochrome P450	TMP Concentration	1-NO-TMP	3-NO-TMP	3'-desmethyl-TMP	4'-desmethyl-TMP	Cα-OH-TMP	Cα-NAC-TMP
1A2	**(5uM)**	0.444	**0.710****	**0.578***	0.437	0.247	0.232
	(50uM)	0.434	**0.785****	**0.555***	0.409	0.235	0.221
2A6	**(5uM)**	**0.633****	0.435	**0.554***	**0.566***	**0.506***	0.493
	(50uM)	**0.587****	0.391	**0.512***	**0.558***	0.488	0.488
2B6	**(5uM)**	**0.499***	0.145	0.055	0.352	**0.521***	**0.510***
	(50uM)	0.404	0.077	0.000	0.316	0.459	0.457
2C8	**(5uM)**	**0.734****	**0.884****	**0.750****	**0.930****	0.302	0.292
	(50uM)	**0.612***	**0.807****	**0.694****	**0.867****	0.303	0.286
2C9	**(5uM)**	**0.742****	**0.629****	**0.873****	**0.759****	**0.502***	**0.499***
	(50uM)	**0.763****	**0.616***	**0.888****	**0.809****	**0.537***	**0.528***
2C19	**(5uM)**	0.429	0.152	0.145	0.239	**0.500***	**0.502***
	(50uM)	0.379	0.152	0.122	0.255	0.424	0.428
2D6	**(5uM)**	0.110	0.167	0.436	0.190	0.032	0.045
	(50uM)	0.167	0.190	0.481	0.251	0.063	0.055
2E1	**(5uM)**	0.110	0.032	0.226	0.000	0.190	0.192
	(50uM)	0.197	0.000	0.167	0.000	0.237	0.251
2J2	**(5uM)**	**0.510***	0.089	0.438	0.390	**0.548***	**0.571***
	(50uM)	**0.540***	0.095	**0.514***	**0.518***	**0.573***	**0.571***
3A4/5	**(5uM)**	**0.853****	0.148	0.399	**0.509***	**0.991****	**0.990****
	(50uM)	**0.905****	0.138	0.466	**0.632***	**0.994****	**0.995****
4A11	**(5uM)**	0.389	**0.512***	0.458	0.489	0.164	0.179
	(50uM)	0.423	**0.544***	**0.511***	**0.511***	0.217	0.219

* significant at $P < 0.05$, ** significant at $P < 0.01$

Inhibition studies were conducted to corroborate the identities of the enzymes involved in the formation of TMP *N*-oxides. As shown in Figure 3, panel C, the formation of 1-NO-TMP was inhibited markedly (greater than 20% inhibition) and in a concentration dependent manner by thiotepa (CYP2B6 inhibitor) and ketoconazole (CYP3A inhibitor). However, cDNA-expressed CYP2B6 did not appear to catalyze 1-NO-TMP formation, nor was CYP2B6 activity correlated significantly with 1-NO-TMP formation in the panel of HLMs, suggesting that CYP2B6 may not be a major catalyst of this reaction. α-Naphthoflavone (CYP1A inhibitor) was the only inhibitor examined that was found to inhibit 3-NO-TMP formation. The other competitive P450 inhibitors resulted in little or no inhibition of either 1-NO-TMP or 3-NO-TMP formation supporting the assertion that 1-NO-TMP and 3-NO-TMP formation are catalyzed primarily by CYP3A4 and CYP1A2, respectively.

TMP Demethylation (3' and 4'-desmethyl-TMP)

Several heterologously expressed P450 isoforms examined in this study demonstrated the capability to catalyze the formation of 3' and 4'-desmethyl-TMP at 5μM TMP (Figure 4, panel A). At a substrate concentration of 50μM, both CYP2C19 and CYP2D6 also catalyzed the 3'-demethylation (data not shown).

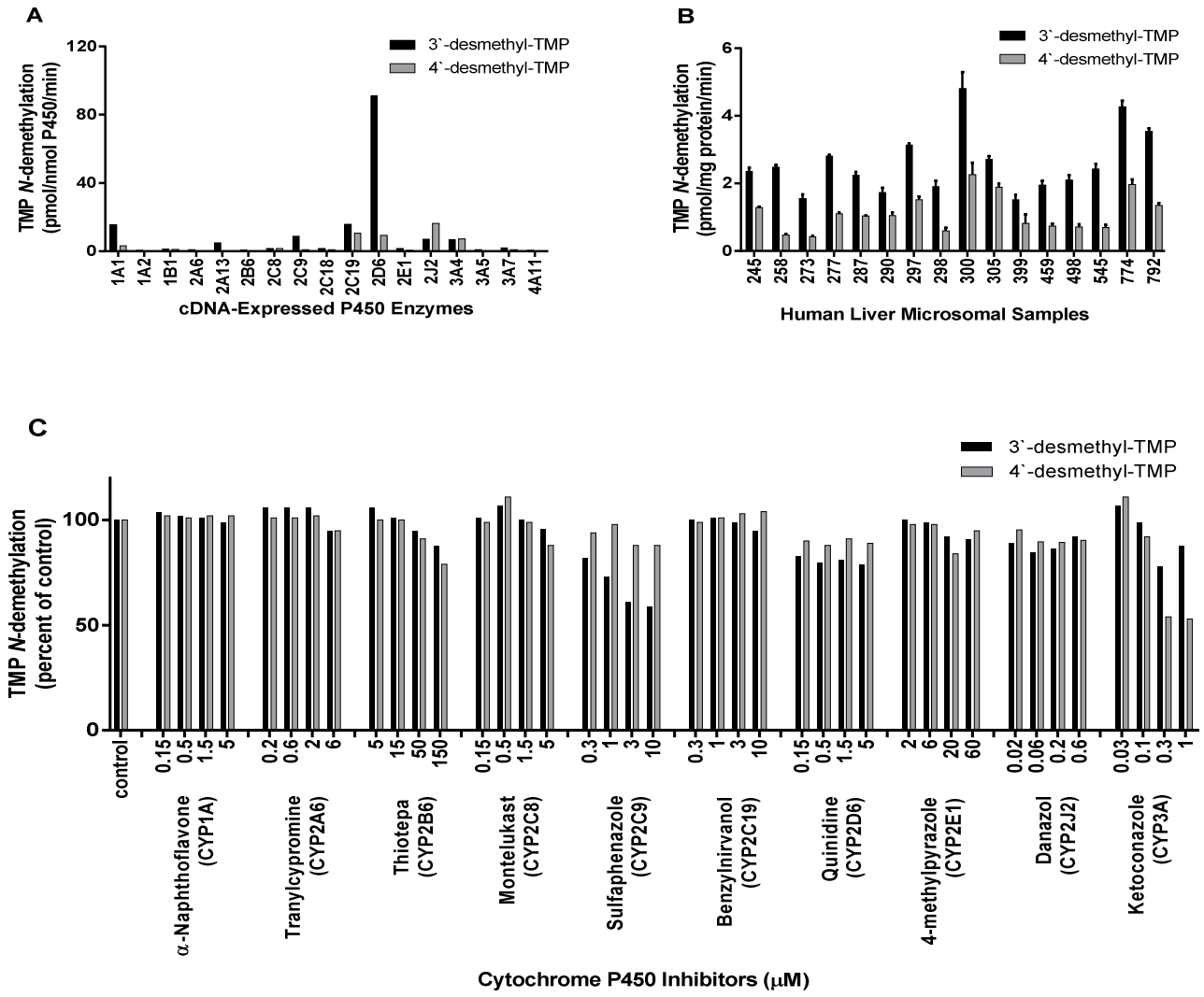

Figure 4. Demethylation of TMP to primary metabolites.

The panel of HLMs was again used to examine demethylated TMP primary metabolite formation and variability was appreciated in rate formation among the sixteen different preparations (Figure 2, panel B; Figure 4, panel B). At a substrate concentration of 5μM, there was nearly 3-fold variation in 3'-desmethyl-TMP formation ranging from 1.5 ± 0.14 to 4.8 ± 0.49 pmol/mg protein/min as compared to 5-fold variation in 4'-desmethyl-TMP formation ranging from 0.4 ± 0.02 to 2.3 ± 0.35 pmol/mg protein/min. The sample-to-sample variation in rate formation of 3' and 4'-desmethyl-TMP correlated ($P< 0.01$) with CYP2C8 and CYP2C9 activities (Table 2).

HLMs were incubated with 50 μM TMP and individual select P450 inhibitors at four concentrations (Figure 4, panel C). The formation of 3'-desmethyl-TMP was significantly inhibited by sulfaphenazole (CYP2C9 inhibitor) while only ketaconazole (CYP3A inhibitor) inhibited 4'-desmethyl-TMP metabolite formation. The other competitive P450 inhibitors resulted in little or no inhibition. Kinetics studies were subsequently performed with CYP3A and CYP2C9 to determine apparent K_m and V_{max} values (Table 1). The apparent K_m values for the formation of 3' and 4'-desmethyl-TMP by the heterologously expressed CYP2C9 and CYP3A4 were nearly 2-fold higher as compared to value calculated from the pooled HLMs. CYP2C9 was the primary pathway for 3'-desmethyl-TMP formation while CYP3A4 contributed to formation of all metabolites except 1-NO-TMP. These cumulative data suggested CYP2C9 catalyzed 3'-desmethylation and CYP3A4 catalyzed 4'-desmethylation.

TMP α-bridge Oxidation (Cα-OH-TMP and Cα-NAC-TMP)

The individual incubations with one of seventeen cDNA-expressed human P450 enzymes were conducted. CYP1A1 and CYP3A had the capability of catalyzing Cα-OH-TMP while CYP3A catalyzed Cα-NAC-TMP (Figure 5, panel A).

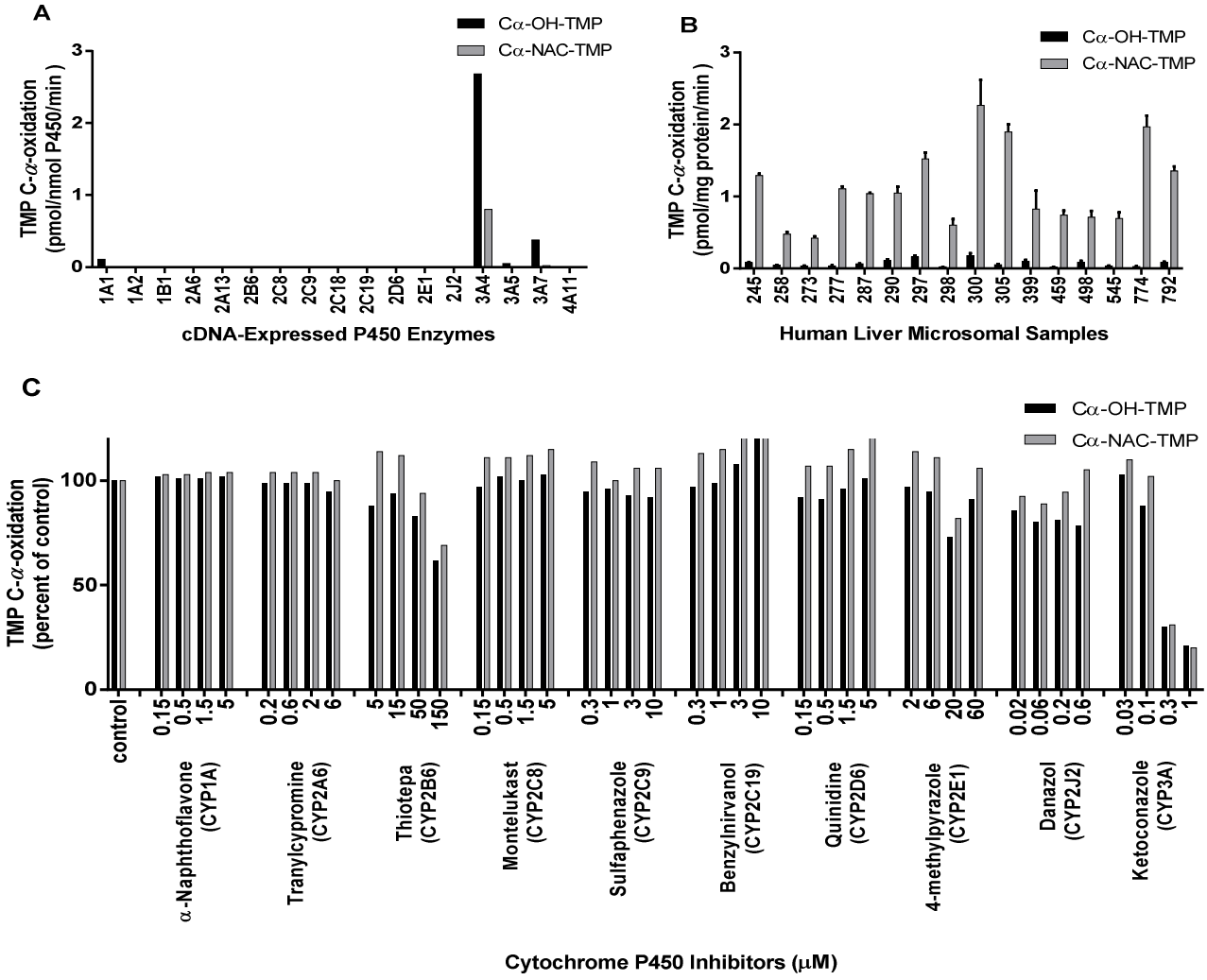

Figure 5. Cα-oxidation of TMP to primary metabolites.

The panel of 16 HLMs was used to examine TMP metabolites formed by oxidative biotransformation at the α-bridge carbon. Considerable variability in rate formation was observed among the sixteen different preparations (Figure 2, panel C; Figure 5, panel B). At the 5μM substrate level, there was nearly 10-fold variation in Cα-OH-TMP ranging from 0.02 ± 0.004 to 0.18 ± 0.03 pmol/mg protein/min and 17-fold variation in Cα-NAC-TMP ranging from 0.007 ± 0.006 to 0.12 ± 0.07 pmol/mg protein/min formation, respectively. The sample-to-sample variation in the rates of Cα-OH-TMP and Cα-NAC-TMP formation significantly correlated only with CYP3A4/5 ($P < 0.01$) (Table 2). Furthermore, inhibition studies revealed that the formation of Cα-OH-TMP and Cα-NAC-TMP were significantly inhibited by ketoconazole (CYP3A inhibitor) (Figure 5, panel C).

DISCUSSION

Comprehensive characterization of the human P450 enzymes involved in TMP biotransformation has not been reported. Only one previous *in* vitro study (Damsten et al.) has provided insight into the enzymes involved in the formation of TMP metabolites. However, Damsten et al implicated the P450 enzymes involved in TMP metabolic pathways based solely on experiments conducted with heterologously expressed P450 enzymes, without additional kinetic, correlation or inhibition approaches that are needed to more completely determine the P450 enzymes involved in TMP biotransformation. Therefore, the present study was undertaken to further define the role that P450s play in the primary metabolism of TMP, with particular interest in the P450s responsible for metabolites observed *in vivo*, and especially the formation of Cα-NAC-TMP, as this is a postulated product of a reactive intermediate. Furthermore, the primary metabolites, 3'-desmethyl and 4'-desmethyl-TMP, may serve as potential precursors to

reactive metabolites because both 3' and 4'-desmethyl-NAC-TMP adducts have been identified *in vitro* and *in vivo*.(van Haandel et al., 2014)

Many of the results from the current study corroborate the observations noted by Damsten et al.(Damsten et al., 2008). CYP3A4 was identified as the major contributor to Cα-NAC-TMP formation. We also identified CYP3A4 as the primary catalyst of Cα-NAC-TMP formation based on the results of correlation and inhibition studies, as well as the results of experiments with heterologously expressed P450 enzymes. The evidence implicating CYP3A4 as the primary catalyst of Cα-NAC-TMP formation is compelling: of the cDNA-expressed P450s examined, CYP3A4 catalyzed Cα-NAC-TMP formation, CYP3A4/5 activity was significantly correlated with the rate of Cα-NAC-TMP formation in the panel of HLMs, and the potent CYP3A inhibitor, ketoconazole, inhibited Cα-NAC-TMP formation in a concentration dependent manner. CYP3A4 also appears to be a major contributor of Cα-OH-TMP formation based on similar findings. Interestingly, CYP3A5 and CYP3A7, enzymes that are expressed in hepatic tissue (Hakkola et al., 1998) also catalyzed Cα-OH-TMP formation. CYP3A7 expression dominates in the fetal and neonatal liver, but rapidly decreases in activity postnatally while CYP3A5 expression is relatively low when compared to other P450s, but constant.(Hines, 2007) Thiotepa, a CYP2B6 inhibitor, inhibited Cα-OH-TMP formation in a concentration dependent manner, but to a lesser extent, than did the CYP3A inhibitor, ketoconazole. Interestingly, heterologously expressed CYP2B6 did not appear to catalyze Cα-OH-TMP formation. At the higher concentrations of the inhibitor, thiotepa, there is potential for less selectivity. This may result in partial inhibition of CYP3A leading to some reduction of metabolite formation not related to CYP2B6 activity.

CYP3A4 also appears to play a major role in the formation of the metabolite 4'-desmethyl TMP. Although several heterologously expressed P450s, including 2C19, 2D6, 2J2 and 3A4, demonstrated the capability to catalyze TMP 4'-demethylation , the only effective inhibitor of TMP 4-demethylation examined in HLMs was the CYP3A inhibitor, ketoconazole, which inhibited ~50% of TMP 4'-demethylase activity. Several P450 activities correlated with 4'-desmethyl TMP formation in the panel of HLMs suggesting that although CYP3A4 appears to be a major contributor to 4'-desmethyl TMP formation, it is likely that other P450 enzymes may contribute to the formation of this metabolite at therapeutically relevant concentrations of TMP.

Although heterologously-expressed CYP2D6 was the most prolific enzyme catalyzing the formation of the most abundant metabolite in our experiments, i.e., 3'-desmethyl TMP, corroborating the observation by Damsten et al.(Damsten et al., 2008) the CYP2D6 inhibitor quinidine caused no appreciable inhibition of TMP 3'-demethylation and the CYP2D6 activity of the HLM panel poorly correlated with rates of TMP 3'-demethylation ($r = 0.481$). In contrast, heterologously expressed CYP2C9 catalyzed a much lower rate of TMP 3'-demethylation than did CYP2D6, but CYP2C9 appeared to play a major role in TMP 3'-demethylation in microsomal systems based on the observations that the CYP2C9 inhibitor, sulfaphenazole, substantially inhibited the formation of 3'-desmethyl TMP in pooled HLMs and the rate of 3'-desmethyl TMP formation significantly correlated with CYP2C9 and CYP2C8 activities (which are co-regulated) in the panel of HLMs. Because the activities of individual heterologously-expressed P450s are dependent on a number of factors including co-expression of cytochrome P450 reductase and in some cases cytochrome b5, lipid membrane composition, etc., the use of heterologously expressed P450 enzymes usually is reserved for identification of isoforms capable of catalyzing a particular reaction.(Parkinson, 1996) The current example provides a

case in point. Although CYP2D6 had the capability of 3'-demethylation with the heterologously expressed enzyme, CYP2D6 has a relative low content and activity as compared to other enzymatic activity, suggesting that in systems in which multiple enzymes are expressed (i.e. HLMs, *in vivo*), CYP2D6 activity may be overshadowed by other enzymes as the amount of CYP2D6 accounts for a relatively small portion of total P450 in the liver. (Venkatakrishnan et al., 2000)

Our results suggest that P450s 2C9 and 3A4 are key enzymes in the biotransformation pathways responsible for metabolic clearance of TMP and the formation of reactive intermediates. SNPs present in *CYP2C9* and *CYP3A4* genes have the potential to contribute to inter-individual differences in drug disposition. (Kirchheiner and Brockmoller, 2005; Werk and Cascorbi, 2014). Hence, it is reasonable to expect that genotypic variation in *CYP2C9* and *CYP3A4* has the potential to alter the balance between bioactivation and detoxification impacting the relative abundance of reactive and stable TMP metabolites. Further studies assessing *in vivo* TMP bioactivation are needed to better understand the extent and variability of TMP bioactivation in humans. As observed in our *in vitro* experiments, there was substantial variability in the rate of TMP Cα-carbon bioactivation; bioactivation and detoxification via Cα-NAC-TMP formation varied by more than 15-fold. In addition, factors that determine which pathway TMP Cα-carbon oxidation intermediates commit to Cα-OH-TMP or Cα-NAC-TMP are currently unknown. The ratio of Cα-OH-TMP or of Cα-NAC-TMP varied between individual samples, indicating that additional factors are likely involved, otherwise one would expect a consistent ratio if a stoichiometric relationship was the only determining factor. Presumably, Cα-OH-TMP and Cα-NAC-TMP share the same intermediate, yet factors determining whether a reactive intermediate is formed resulting in a NAC adduct versus a stable metabolite (Cα-OH-

TMP) remain unclear. Further studies are necessary to identify determinants resulting in the variability of the imino-quinone intermediate formation as this may serve as a potential risk factor for IADR development. It is feasible that variability in CYP3A4 activity relative to other P450s determines the extent of primary TMP bioactivation *in vivo* and further studies are underway to assess the extent of primary TMP metabolism variability *in vivo*. Factors modulating activity of these contributing enzymes may affect the risk of ADRs.(Gill et al., 1999)

Interestingly, previous data propose that SMX undergoes CYP2C9-mediated bioactivation to a hydroxylamine. This hydroxylamine undergoes subsequent auto-oxidation resulting in a reactive nitroso intermediate that can form haptenated cellular proteins capable of triggering a cellular immune response.(Callan et al., 2009; Naisbitt et al., 2002) The results of the present study demonstrate that CYP2C9 contributes to formation of the most abundant primary TMP metabolite (3'-desmethyl TMP) *in vitro*. Consequently, the potential exists for either TMP or SMX to directly influence the extent of metabolism and possible bioactivation of the other component when administered concomitantly at a combined fixed dose. For example, an individual who extensively metabolizes TMP to the 3'-desmethyl TMP metabolite could conceivably experience a relative decrease in the amount of SMX hydroxylamine that is formed. There is no evidence of mechanism based inhibition of either trimethoprim or sulfamethoxazole; however the extent of metabolism potentially impacting bioactivation of the other component has not been evaluated. (Wen et al., 2002)

Our current work only characterizes the role that P450 enzymes play in the primary biotransformation pathways of TMP. Detection of 4'-desmethyl TMP glutathione or NAC adducts *in vitro* and *in vivo* implies that 4'-desmethyl TMP undergoes a further oxidation step

presumably through a quinine methide intermediate (Leblanc et al., 2010; van Haandel et al., 2014). Subsequent bioactivation of a stable primary metabolite has been attributed to potential additional pathways resulting in IADRs with commonly implicated drugs such as phenytoin and carbamazepine.(Cuttle et al., 2000; Pearce et al., 2008)

In summary, our *in vitro* studies implicate CYP3A4 as the predominant cytochrome P450 enzyme involved in the direct formation of a reactive metabolite (i.e. Cα-NAC-TMP) from TMP. In addition, CYP 3A4 plays a major role in the generation of 4'-desmethyl TMP, which is believed to be a precursor in a second bioactivation pathway. Characterization of the isoforms responsible for secondary TMP bioactivation is critical to understand all potential sources of inter-individual variation involved in the generation of reactive intermediates capable of forming haptenated proteins. Although TMP has historically been overlooked as a probable contributor of IADRs; evidence of TMP bioactivation suggests that it too may contribute to these well-recognized, unpredictable reactions associated with TMP-SMX. Therefore, a better understanding of bioactivation may potentially providing insight in identifying those at risk of developing an IADR prior to its occurrence.

REFERENCES

Brooks, MA, JA De Silva andL D'Aroconte (1973) Determination of trimethoprim and its N-oxide metabolites in urine of man, dog, and rat by differential pulse polarography. *J Pharm Sci* **62:** 1395-7.

Callan, HE, RE Jenkins, JL Maggs, SN Lavergne, SE Clarke, DJ Naisbitt andBK Park (2009) Multiple adduction reactions of nitroso sulfamethoxazole with cysteinyl residues of peptides and proteins: implications for hapten formation. *Chem Res Toxicol* **22:** 937-48.

Clarkson, A andI Choonara (2002) Surveillance for fatal suspected adverse drug reactions in the UK. *Archives of Disease in Childhood* **87:** 462-466.

Copp, HL, DJ Shapiro andAL Hersh (2011) National ambulatory antibiotic prescribing patterns for pediatric urinary tract infection, 1998-2007. *Pediatrics* **127:** 1027-33.

Cuttle, L, AJ Munns, NA Hogg, JR Scott, WD Hooper, RG Dickinson andEM Gillam (2000) Phenytoin metabolism by human cytochrome P450: involvement of P450 3A and 2C forms in secondary metabolism and drug-protein adduct formation. *Drug Metab Dispos* **28:** 945-50.

Damsten, MC, JS de Vlieger, WM Niessen, H Irth, NP Vermeulen andJN Commandeur (2008) Trimethoprim: novel reactive intermediates and bioactivation pathways by cytochrome p450s. *Chem Res Toxicol* **21:** 2181-7.

Gill, HJ, JF Tjia, NR Kitteringham, M Pirmohamed, DJ Back andBK Park (1999) The effect of genetic polymorphisms in CYP2C9 on sulphamethoxazole N-hydroxylation. *Pharmacogenetics* **9:** 43-53.

Hakkola, J, E Tanaka andO Pelkonen (1998) Developmental expression of cytochrome P450 enzymes in human liver. *Pharmacol Toxicol* **82:** 209-17.

Hawkins, T, JM Carter, KR Romeril, SR Jackson andGJ Green (1993) Severe trimethoprim induced neutropenia and thrombocytopenia. *N Z Med J* **106:** 251-2.

Hersh, AL, HF Chambers, JH Maselli andR Gonzales (2008) National trends in ambulatory visits and antibiotic prescribing for skin and soft-tissue infections. *Arch Intern Med* **168:** 1585-91.

Hines, RN (2007) Ontogeny of human hepatic cytochromes P450. *J Biochem Mol Toxicol* **21:** 169-75.

Hoppu, K andP Arjomaa (1984) Difference in trimethoprim pharmacokinetics between children and adults. *Chemotherapy* **30:** 283-7.

Kirchheiner, J andJ Brockmoller (2005) Clinical consequences of cytochrome P450 2C9 polymorphisms. *Clin Pharmacol Ther* **77:** 1-16.

Lai, WG, N Zahid andJP Uetrecht (1999) Metabolism of trimethoprim to a reactive iminoquinone methide by activated human neutrophils and hepatic microsomes. *J Pharmacol Exp Ther* **291:** 292-9.

Leblanc, A, TC Shiao, R Roy andL Sleno (2010) Improved detection of reactive metabolites with a bromine-containing glutathione analog using mass defect and isotope pattern matching. *Rapid Commun Mass Spectrom* **24:** 1241-50.

Manchanda, T, D Hess, L Dale, SG Ferguson andMJ Rieder (2002) Haptenation of sulfonamide reactive metabolites to cellular proteins. *Mol Pharmacol* **62:** 1011-26.

Mofenson, LM, MT Brady, SP Danner, KL Dominguez, R Hazra, E Handelsman, P Havens, S Nesheim, JS Read, L Serchuck, R Van Dyke, C Centers for Disease, Prevention, H National Institutes of, HIVMAotIDSo America, S Pediatric Infectious Diseases andP

American Academy of (2009) Guidelines for the Prevention and Treatment of Opportunistic Infections among HIV-exposed and HIV-infected children: recommendations from CDC, the National Institutes of Health, the HIV Medicine Association of the Infectious Diseases Society of America, the Pediatric Infectious Diseases Society, and the American Academy of Pediatrics. *MMWR Recomm Rep* **58:** 1-166.

Mortimer, NJ, MR Bermingham, SJ Chapple andMJ Sladden (2005) Fatal adverse drug reaction to trimethoprim. *Aust Fam Physician* **34:** 345-6.

Naisbitt, DJ, J Farrell, SF Gordon, JL Maggs, C Burkhart, WJ Pichler, M Pirmohamed andBK Park (2002) Covalent binding of the nitroso metabolite of sulfamethoxazole leads to toxicity and major histocompatibility complex-restricted antigen presentation. *Mol Pharmacol* **62:** 628-37.

Nwokolo, C, L Byrne andKJ Misch (1988) Toxic epidermal necrolysis occurring during treatment with trimethoprim alone. *Br Med J (Clin Res Ed)* **296:** 970.

Parkinson, A (1996) Biotransformation of xenobiotics. CD Klaassen (Ed.), Casarett and Doull's Toxicology. *McGraw-Hill, New York* 113-186.

Pearce, RE, W Lu, Y Wang, JP Uetrecht, MA Correia andJS Leeder (2008) Pathways of carbamazepine bioactivation in vitro. III. The role of human cytochrome P450 enzymes in the formation of 2,3-dihydroxycarbamazepine. *Drug Metab Dispos* **36:** 1637-49.

Roujeau, JC, JP Kelly, L Naldi, B Rzany, RS Stern, T Anderson, A Auquier, S Bastuji-Garin, O Correia, F Locati andet al. (1995) Medication use and the risk of Stevens-Johnson syndrome or toxic epidermal necrolysis. *N Engl J Med* **333:** 1600-7.

Rylance, GW, RH George, DE Healing andDG Roberts (1985) Single dose pharmacokinetics of trimethoprim. *Arch Dis Child* **60:** 29-33.

Sigel, CW, ME Grace andCA Nichol (1973) Metabolism of trimethoprim in man and measurement of a new metabolite: a new fluorescence assay. *J Infect Dis* **128:** Suppl:580-3 p.

van Haandel, L, JL Goldman, RE Pearce andJS Leeder (2014) Urinary biomarkers of trimethoprim bioactivation in vivo following therapeutic dosing in children. *Chem Res Toxicol* **27:** 211-8.

Venkatakrishnan, K, LL von Moltke, MH Court, JS Harmatz, CL Crespi andDJ Greenblatt (2000) Comparison between cytochrome P450 (CYP) content and relative activity approaches to scaling from cDNA-expressed CYPs to human liver microsomes: ratios of accessory proteins as sources of discrepancies between the approaches. *Drug Metab Dispos* **28:** 1493-504.

Wen, X, JS Wang, JT Backman, J Laitila andPJ Neuvonen (2002) Trimethoprim and sulfamethoxazole are selective inhibitors of CYP2C8 and CYP2C9, respectively. *Drug Metab Dispos* **30:** 631-5.

Werk, AN andI Cascorbi (2014) Functional gene variants of CYP3A4. *Clin Pharmacol Ther* **96:** 340-8.

APPENDIX:

Figure 1. Metabolic scheme for the conversion of TMP to its primary oxidative metabolites.

Figure 2. Variability in the rate of formation of primary trimethoprim formation. A panel of commercially available HLMs prepared from 16 individual donors was examined to determine the ability of HLMs to catalyze primary TMP metabolites. Sample to sample variability in metabolite formation is demonstrated: Panel A exhibits TMP *N*-oxidation (1 and 3-NO-TMP), Panel B shows TMP Demethylation (3' and 4'-desmethyl-TMP), and TMP Cα-oxidation (Cα-OH-TMP and Cα-NAC-TMP) is shown in Panel C.

Figure 3. *N*-oxidation of TMP to primary metabolites. Panel A: 1- and 3-NO-TMP formation by human cDNA-expressed P450 enzymes. TMP (5 μM) was incubated with cDNA-expressed P450 enzymes as described under materials and methods. Rates shown are corrected for rates from microsomes containing vectors alone. Each bar represents the mean of the duplicate incubations. Panel B: Sample-to-sample variation in the rates of TMP 1- and 3 *N*-oxidation by HLMs at a substrate concentration of 5 μM. Each bar represents the mean of the triplicate experiments ± S.D. Panel C: Effects of various P450 isoform-selective inhibitors on the formation of 1- and 3-NO-TMP by pooled HLMs at a substrate concentration of 50 μM, as described under Material and Methods. Each bar represents the mean of the triplicate incubations. Uninhibited mean rates of 1- and 3-NO-TMP formation were 205 and 40 pmol/mg protein/min, respectively.

Figure 4. Demethylation of TMP to primary metabolites. Panel A: 3' and 4'-desmethyl-TMP formation by human cDNA-expressed P450 enzymes. TMP (5 μM) was incubated with cDNA-expressed P450 enzymes as described under materials and methods. Rates shown are corrected

for rates from microsomes containing vectors alone. Each bar represents the mean of the duplicate incubations. Panel B: Sample-to-sample variation in the rates of TMP 3' and 4'-desmethyl-TMP by HLMs at a substrate concentration of 5 μM. Each bar represents the mean of the triplicate experiments ± S.D. Panel C: Effects of various P450 isoform-selective inhibitors on the formation of 3' and 4'-desmethyl-TMP by pooled HLMs at a substrate concentration of 50 μM, as described under Material and Methods. Each bar represents the mean of the triplicate incubations. Uninhibited rates of 3' and 4'-desmethyl-TMP formation were 1202 and 731 pmol/mg protein/min, respectively.

Figure 5. Cα-oxidation of TMP to primary metabolites. Panel A: Cα-OH-TMP and Cα-NAC-TMP formation by human cDNA-expressed P450 enzymes. TMP (5 μM) was incubated with cDNA-expressed P450 enzymes as described under materials and methods. Rates shown are corrected for rates from microsomes containing vectors alone. Each bar represents the mean of the duplicate incubations. Panel B: Sample-to-sample variation in the rates of Cα-OH-TMP and Cα-NAC-TMP formation by HLMs at a substrate concentration of 5 μM. Each bar represents the mean of the triplicate experiments ± S.D. Panel C: Effects of various P450 isoform-selective inhibitors on the formation of Cα-OH-TMP and Cα-NAC-TMP by pooled HLMs at a substrate concentration of 50 μM, as described under Material and Methods. Each bar represents the mean of the triplicate incubations. Uninhibited rates of Cα-OH-TMP and Cα-NAC-TMP formation were 116 and 54 pmol/mg protein/min, respectively.